

# Dysregulated Bone Morphogenetic Protein Signaling in Monocrotaline-Induced Pulmonary Arterial Hypertension

Rory E. Morty, Bozena Nejman, Grazyna Kwapiszewska, Matthias Hecker, Anka Zakrzewicz, Fotini M. Kouri, Dorothea M. Peters, Rio Dumitrascu, Werner Seeger, Petra Knaus, Ralph T. Schermuly, Oliver Eickelberg

**Background**—Mutations in the *bmpr2* gene, encoding the type II bone morphogenetic protein (BMP) receptor, have been identified in patients with pulmonary arterial hypertension (PAH), implicating BMP signaling in PAH. The aim of this study was to assess BMP signaling and its physiological effects in a monocrotaline (MCT) model of PAH.

**Methods and Results**—Expression of BMP receptors Ib and II, and Smads 4, 5, 6, and 8, was downregulated in lungs but not kidneys of MCT-treated rats. Smad1 phosphorylation and expression of BMP/Smad target genes *id1* and *id3* was also reduced, although ERK1/2 and p38<sup>MAPK</sup> phosphorylation remained unaffected. BMP receptor and Smad expression, Smad1 phosphorylation, and induction of the BMP/Smad-responsive element of the *id1* promoter were reduced in pulmonary artery smooth muscle cells (PASMCs) from MCT-treated rats. As a consequence of impaired BMP/Smad signaling, PASMCs from MCT-treated rats were resistant to apoptosis induced by BMP-4 and BMP-7, and were also resistant to BMP-4 antagonism of proliferation induced by platelet-derived growth factor.

**Conclusion**—BMP signaling and BMP-regulated physiological phenomena are perturbed in MCT-treated rats, lending solid support to the proposed roles for BMP signaling in the pathogenesis of human PAH. (*Arterioscler Thromb Vasc Biol.* 2007;27:1072-1078.)

**Key Words:** bone morphogenetic proteins ■ monocrotaline ■ pulmonary arterial hypertension ■ Smad ■ vascular remodeling ■ VSMC proliferation

Pulmonary arterial hypertension (PAH) is a rare and often fatal disorder of unknown etiology that occurs either sporadically (idiopathic PAH [IPAH]) or as an inherited form (familial PAH [FPAH]), and is characterized by increased pulmonary vascular resistance, which develops as a consequence of vasoconstriction, thrombosis, and vascular remodeling.<sup>1,2</sup> A key pathological feature of IPAH is remodeling of precapillary pulmonary arteries, where increased proliferation of pulmonary artery smooth muscle cells (PASMCs) and disordered proliferation of endothelial cells results in medial hypertrophy and concentric obliteration of the lumen.<sup>2,3</sup> Decreased intraluminal space increases the pulmonary vascular resistance, causing right heart failure. Although the etiology of IPAH is not clear, several lines of evidence have implicated bone morphogenetic protein (BMP) receptors, which are members of the transforming growth factor (TGF)- $\beta$  receptor superfamily.<sup>4,5</sup>

The BMP ligands bind to heteromeric complexes of their type I BMP receptors, Bmpr1a (also called ALK-3) and Bmpr1b (also called ALK-6), and the type II BMP receptor (Bmpr2). Signaling proceeds by phosphorylation of the intracellular signaling molecules, Smad1, Smad5, and Smad8,

which together with Smad4 are translocated into the nucleus, where they regulate transcription of BMP/Smad-responsive genes,<sup>6</sup> or via Smad-independent pathways involving the MAP kinases p38<sup>MAPK</sup> and ERK1/2.<sup>5,6</sup>

Mutations in the *bmpr2* gene have been identified in more than 50% of FPAH patients and in 10% to 25% of IPAH patients.<sup>7,8</sup> These mutations disrupt BMP/Smad-mediated signaling,<sup>9</sup> and potentiate BMP/MAP kinase signaling.<sup>10</sup> Reduced levels of Bmpr1a<sup>11</sup> and Bmpr2<sup>12</sup> were observed in the lungs of patients with FPAH and IPAH, and in patients with PAH secondary to thromboembolic disease, ventricular septal defects, or mitral valve regurgitation. These data suggest a role for BMP signaling in PAH and are supported by observations in experimental animals.<sup>13–15</sup> Two animal models of IPAH are currently in routine use: one using exposure to hypoxia, and the other using the pyrrolizidine alkaloid monocrotaline (MCT).<sup>16,17</sup> In both instances, right ventricular hypertrophy and PAH develop. Despite widespread use of the MCT model, no study to date has addressed a role for BMP signaling in MCT-induced PAH. The data that we present in this article illustrate that the BMP/Smad signaling axis in the lung is perturbed in MCT-induced PAH and that this per-

Original received October 9, 2006; final version accepted February 22, 2007.

From the Department of Internal Medicine (R.M., B.N., G.K., M.H., A.Z., F.K., D.P., R.D., W.S., R.S., O.E.), University of Giessen Lung Center, Justus Liebig University, Giessen; and the Institute of Chemistry and Biochemistry (P.K.), Free University of Berlin, Germany.

Correspondence to Rory E. Morty, Department of Internal Medicine, University of Giessen Lung Center, Justus Liebig University, Aulweg 123 (Raum 6-11), D-35392 Giessen, Germany. E-mail rory.morty@innere.med.uni-giessen.de

© 2007 American Heart Association, Inc.

*Arterioscler Thromb Vasc Biol.* is available at <http://www.atvbaha.org>

DOI: 10.1161/ATVBAHA.107.141200

turbed signaling has functional consequences for the maintenance of PASMCM cell mass, and hence vascular resistance, associated with MCT-induced PAH. As such, these data lend strong support to the proposed roles for dysregulated BMP signaling in the pathogenesis of IPAH.

## Methods

### Animals and Hemodynamics

The government of the State of Hessen approved all animal procedures. Pulmonary hypertension was induced in adult male Sprague-Dawley rats (15 per experimental group; Charles River Laboratories) by a single intraperitoneal injection of MCT (60 mg·kg<sup>-1</sup>; Sigma). Animal handling, measurement of hemodynamic parameters, and lung extraction were conducted as described previously.<sup>18,19</sup>

### RNA Isolation, Semi-Quantitative PCR, and Real-Time PCR

Total RNA was isolated from fresh lung tissue using a Qiagen RNeasy kit (Qiagen). Total RNA was screened for mRNA encoding genes of interest by semi-quantitative RT-PCR<sup>20</sup> using the intron-spanning primers indicated in supplemental Table I (available online at <http://atvb.ahajournals.org>). Cycle numbers lie in the logarithmic phase for each PCR. Quantitative changes in gene expression were also analyzed by quantitative real-time PCR (RNA samples from 5 different animals per group, each sample assessed in duplicate) by the  $\Delta\Delta C_t$  method,<sup>21</sup> using primer pairs indicated in supplemental Table I. The ubiquitously-expressed hydroxymethylbilane synthase (*hmbg*) gene was used as a reference.

### Protein Isolation and Immunoblotting

Protein extraction from rat lungs, kidneys, and cultured PASMCMs and gel electrophoresis and immunoblotting were performed as described previously.<sup>20,22</sup> Blots were probed with rabbit anti-Smad1, anti-p44/42, anti-p38 p38<sup>MAPK</sup>, anti-phospho-p38 p38<sup>MAPK</sup>(Thr180/Tyr182), or mouse anti-phospho-p44/42(Thr202/Tyr204) (Cell Signaling Technology), rabbit anti-Smad5 (Zymed), goat anti-Smad8 and mouse anti-Acvr2a (R&D Systems), rabbit anti-phospho-Smad1(Ser463/ser465) and anti-Smad4 (Upstate), and rabbit anti-Avcr1 (Santa Cruz Biotechnology). Rabbit polyclonal antibodies against Bmpr1a, Bmpr1b, and Bmpr2 have been described previously.<sup>23</sup> None of the antibodies used exhibit cross-reaction with related proteins. Mouse anti- $\beta$ -actin or anti- $\alpha$ -tubulin (1:1000; Cell Signaling Technology) served as a loading control. Peroxidase-conjugated secondary antibodies (1:3000 to 1:3500) were from Pierce. Densitometric analysis of protein bands was performed as described previously.<sup>20</sup>

### Immunohistochemistry

Elastin and H&E staining, and expression of BMP receptors, Smads, smooth muscle actin (SMA), von Willebrand factor (vWF), and proliferating cell nuclear antigen (PCNA) was assessed on 3- $\mu$ m tissue sections,<sup>18,19</sup> with mouse anti-SMA (1:850; clone 1A4; Sigma) and anti-vWF (1:800; Dako); rabbit anti-Bmpr1a (1:150), -Bmpr1b (1:150), and -Bmpr2 (1:150)<sup>23</sup>; and rabbit anti-Smad1, -Smad4 (both at 1:50; Upstate) and -PCNA (1:100; Santa Cruz Biotechnology).

### Assessment of Proliferation and Apoptosis of PASMCM

Primary rat PASMCMs were isolated from the second to the fifth branch of the pulmonary artery<sup>19,24</sup> from saline-treated or MCT-treated rats, 4 weeks after treatment. The proliferation of PASMCMs in response to platelet-derived growth factor (PDGF; 20 ng·ml<sup>-1</sup>) applied alone, or together with BMP-4 (20 ng·ml<sup>-1</sup>) was studied in 24-well plates by [<sup>3</sup>H]thymidine incorporation.<sup>24</sup> For assessment of apoptosis, PASMCMs were seeded at 1×10<sup>4</sup> cells per well in chamber slides and grown to  $\approx$ 80% confluence. Quiescent cells (cultured in 0.1% [v/v] FBS for 48 hours) were treated with BMP-4 or -7 (100 ng·ml<sup>-1</sup>; 24 hours), after which cells were fixed and processed,<sup>19</sup> using the terminal deoxynucleotidyl transferase-mediated dUTP

nick end-labeling (TUNEL) reaction with dUTP-fluorescein isothiocyanate (FITC; in situ cell death detection kit; Roche).

### Luciferase Reporter Assay

PASMCMs, seeded in 24-well plates (70% confluent), were transiently transfected with LipofectAMINE (Invitrogen),<sup>25</sup> with pId120, a reporter construct containing a BMP-responsive promoter upstream of a firefly luciferase gene.<sup>26</sup> Alternatively, cells were transfected with pGL3-Basic (containing a promoterless luciferase gene) or pGL3-Control (containing a constitutively-expressed luciferase gene) both from Promega as negative and positive controls, respectively. Cells were incubated with BMP-4 or BMP-7 (20 ng·ml<sup>-1</sup>) for 12 hours. Cells were lysed and processed for determination of firefly luciferase activity as recommended by the manufacturer.

### Statistical Treatment of Data

Data are presented as mean $\pm$ SD. Differences between groups were analyzed by ANOVA and the Student-Newman-Keul post-hoc test for multiple comparisons, with a probability value <0.05 regarded as significant.

## Results

### Induction of PAH and Vascular Remodeling by MCT

Vascular remodeling was evident by thickening of small pulmonary artery vessel walls in rats 4 weeks after MCT administration, together with a significant increase in the right ventricle-to-left ventricle+septum ratio (supplemental Figure IB, ID, and IG, available online at <http://atvb.ahajournals.org>), which was not observed in saline-treated control animals (supplemental Figure IA, IC, and IG). These changes were accompanied by an increase in right ventricular systolic pressure (supplemental Figure IE) and a decrease in the partial pressure of oxygen in arterial blood (supplemental Figure IH), although no change in systemic arterial pressure was observed (supplemental Figure IF).

### Dysregulated Expression of BMP Signaling Machinery in Lungs From MCT-Treated Rats

A moderate to dramatic decrease in the expression of mRNA encoding Bmpr1b, Bmpr2, and Smads 4, 5, 6, and 8 was observed in the lungs, but not the kidneys, of rats 4 weeks after MCT administration, as assessed by semi-quantitative RT-PCR (Figure 1A). Similar data were obtained by real-time RT-PCR (Figure 1B), where a significant reduction in levels of mRNA encoding Bmpr1a, Bmpr2, and Smad4 was observed as early as 2 weeks after MCT administration. Four weeks after MCT administration, levels of mRNA encoding all classical BMP receptors and Smads evaluated, and the alternative BMP receptors Acvr1 and Avcr2a, were significantly decreased, although to varying degrees, relative to saline-treated control rats. Because mast cell chymase (*Cma1*) levels are elevated in the lungs in IPAH patients,<sup>27</sup> and hemoxygenase-1 (*Hmox1*) levels are elevated in the lungs of MCT-treated experimental animals that develop PAH,<sup>28</sup> we also screened *cma1* and *hmox1* mRNA levels as positive controls, and both markers were significantly elevated in the lungs, but not the kidneys, of experimental animals.

Reduced expression of BMP receptors and Smads was confirmed at the protein level by immunoblot (Figure 2A). Quantitation of immunoblot data confirmed a significant decrease in the expression of Bmpr1b and Bmpr2, and Smads

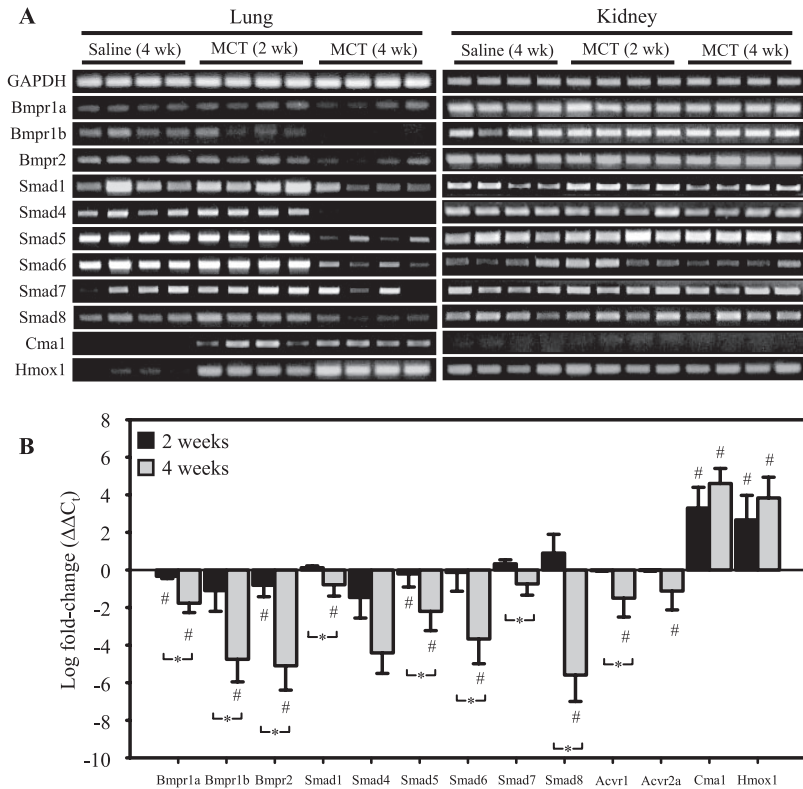


**Figure 1.** Gene expression of BMP signaling machinery in MCT-treated rats, assessed by (A) semi-quantitative and (B) real-time RT-PCR ( $\Delta\Delta C_t$  values: black bars, 2 weeks; gray bars, 4 weeks; relative to saline-treated controls at 4 weeks). wk indicates weeks. # $P < 0.05$  relative to controls; \* $P < 0.05$  between indicated groups.

4, 5, and 8 (supplemental Figure II). Bmpr1a exhibited a trend toward reduced expression; however, this trend did not reach statistical significance, whereas Smad1 levels appeared relatively stable.

On histological examination of lungs of MCT-treated rats, inflammatory infiltrates and vessel wall thickening were uniformly observed (Figure 3). Bmpr1a exhibited a moderate decrease in staining intensity of both the alveolar epithelium (supplemental Figure III) and the smooth muscle layer of large vessels from MCT-treated rats (Figure 3B), compared with material from healthy, saline-treated controls (Figure 3A). A strong reduction in staining was observed for Bmpr1b (Figure 3C and 3D) and Bmpr2 (Figure 3E and 3F). Notably, loss of Bmpr2 staining in the vascular endothelium of large vessels was observed (Figure 3F). In the case of Smad proteins, whereas Smad1 staining appeared relatively unaf-

ected in the airways (supplemental Figure III) and vessels from MCT-treated rats (Figure 3G and 3H), Smad4 staining was dramatically reduced in the airway epithelium (supplemental Figure III) and smooth muscle layer of small vessels of MCT-treated rats (Figure 3I and 3J). These changes in BMP receptor and Smad expression paralleled trends observed in our RT-PCR and immunoblot analyses. Together, these data document a dramatic reduction in the expression of the BMP signaling machinery in the lungs of MCT-treated rats.

### Dysregulated BMP Signaling in Lungs From MCT-Treated Rats

The reduced expression of BMP receptor and Smad proteins observed in the lungs of MCT-treated rats suggested that BMP signaling was most likely also perturbed. Indeed, a dramatic decrease in baseline Smad1 phosphorylation in lung homogenates was observed after MCT-administration (Figure 4A). In contrast, baseline levels of phosphorylated ERK1/2 were only slightly reduced, and levels of phosphorylated p38<sup>MAPK</sup> were unaffected (Figure 4A). Genes encoding the Id family of helix-loop-helix proteins, in particular, Id1, are direct targets of Smad1-dependent BMP signaling,<sup>29</sup> by both BMP-4 and BMP-7.<sup>30</sup> We therefore evaluated expression of the *id1*, *id2*, and *id3* genes as a read-out of BMP/Smad signaling. In line with our earlier observations, the expression of both *id1* and *id3* genes was reduced, as assessed by semi-quantitative RT-PCR (Figure 4B). Further analysis by real-time RT-PCR indicated that *id1* mRNA levels were reduced 2 weeks after MCT-administration, whereas mRNA levels of both *id1* and *id3* were reduced 4 weeks after MCT administration ( $\Delta\Delta C_t$  of  $-4.8$  and  $-2.1$ , respectively; supplemental Figure IV). Taken together, these data demonstrate

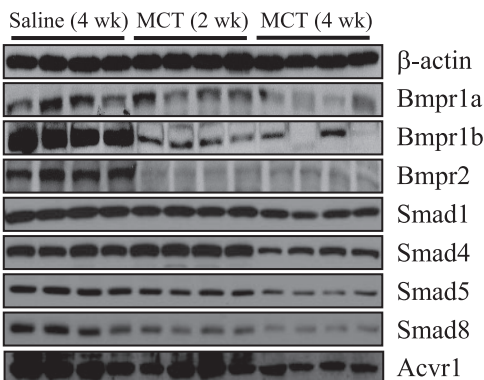


**Figure 2.** Protein expression of BMP signaling machinery in MCT-treated rats assessed by immunoblot. wk indicates weeks.

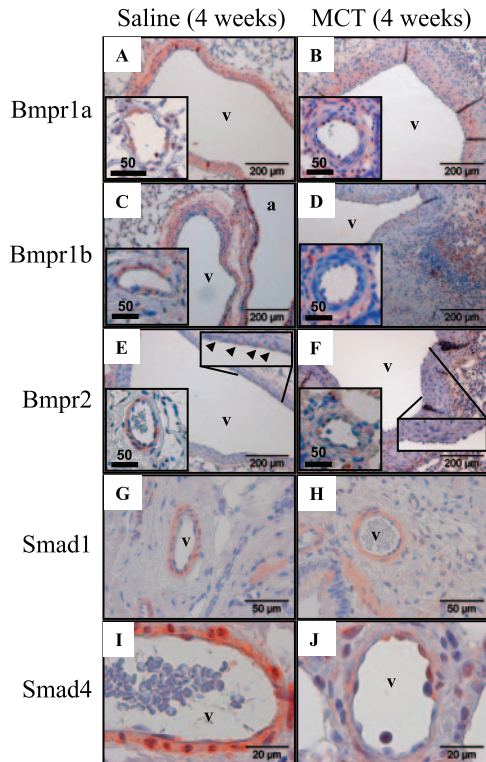


**Figure 3.** Localization of BMP receptors and Smad proteins in lungs from MCT-treated rats. BMP receptors or Smads were localized (red color) in the lungs of saline- and MCT-treated rats. Both large (internal diameter 400 to 800  $\mu\text{m}$ ) and small (internal diameter 150 to 400  $\mu\text{m}$ ; insets) resistance pulmonary arteries are illustrated. In the case of Bmpr2, some aspects have been magnified in the panels. Where necessary, arrowheads indicate staining.

that BMP signaling is impaired in the lungs of MCT-treated rats. This decreased signaling could not be attributed to Smad6, which antagonizes BMP signaling, because levels of mRNA encoding Smad6 were reduced in lungs of MCT-treated rats (Figure 1A and 1B). Given the important and opposing roles of Smad and MAP kinase pathways in regulating cell proliferation, we examined cell proliferation in the lungs of MCT-treated rats using PCNA staining as an indicator of proliferating cells. An increased frequency of proliferating cells was observed in the lungs (Figure 4C, panels a and b), specifically, in the smooth muscle layer of

small resistance arteries (Figure 4C, panels c and d) of MCT-treated rats.

### Dysregulated BMP Signaling in PAMSC From MCT-Treated Rats

The PAMSC is a key player in the pathogenesis of PAH,<sup>1-3</sup> and growth and proliferation of PAMSCs are regulated by BMP ligands.<sup>30,31</sup> Because we observed increased proliferation of PAMSCs in the lungs of MCT-treated rats (Figure 4C), we examined whether PAMSCs from MCT-treated rats exhibited altered BMP signaling. Indeed, levels of mRNA encoding Bmpr1b and Bmpr2 and Smad4 were significantly lower in PAMSCs from MCT-treated rats, whereas levels of mRNA encoding Bmpr1a and Smad1 levels were not significantly altered between control and MCT-treated groups ( $\Delta\Delta C_t$  values between  $-1.8$  and  $-2$ ; Figure 5A).

Whereas Smad1 protein levels were unchanged between PAMSCs from saline- and MCT-treated rats, baseline Smad1 phosphorylation was not evident at all in PAMSCs from MCT-treated rats, although it was evident in PAMSCs from saline-treated rats (Figure 5B). In contrast, ERK1/2 levels and ERK1/2 phosphorylation appeared similar in PAMSCs from both saline- and MCT-treated rats (Figure 5B).

We then transfected a BMP-responsive promoter placed upstream of a firefly luciferase gene on the pId120 reporter plasmid<sup>26</sup> into PAMSCs from saline- and MCT-treated rats. Although this promoter was responsive to stimulation by BMP-4 and BMP-7 in PAMSCs from saline-treated rats, the response was significantly (2- to 4-fold) abrogated in PAMSCs from MCT-treated rats (Figure 5C). Together, these data indicate that signaling by the BMP/Smad axis in PAMSCs from MCT-treated rats is impaired.

Proliferation of PAMSCs isolated from both saline- and MCT-treated rats was stimulated by PDGF (Figure 5D). In PAMSCs from saline-treated rats, this effect was antagonized by BMP-4. However, consistent with impaired BMP/Smad signaling in PAMSCs from MCT-treated rats, BMP-4 did not antagonize PDGF-induced proliferation in PAMSCs from MCT-treated rats (Figure 5D). The induction of apoptosis in PAMSCs by BMP ligands is well documented.<sup>32,33</sup> We therefore assessed the induction of apoptosis in PAMSCs from saline- and MCT-treated rats by BMP ligands. Consistent with the abrogated BMP/Smad signaling we observed in PAMSCs from MCT-treated rats, PAMSCs from MCT-

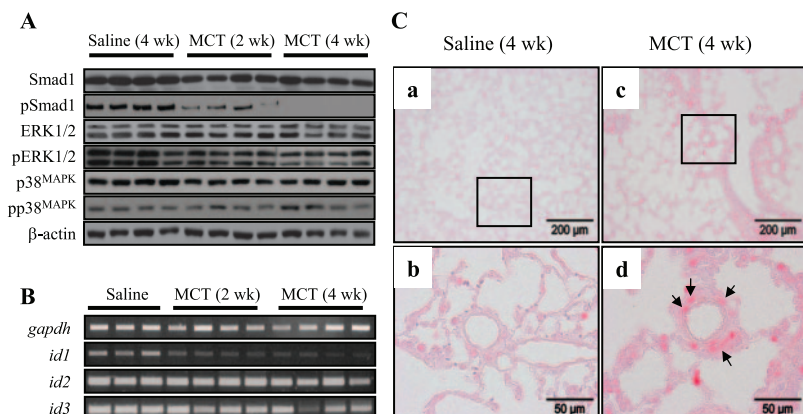


**Figure 4.** BMP signaling in lungs from MCT-treated rats. A, Smad1, ERK, and p38<sup>MAPK</sup> phosphorylation (designated by pSmad1, pERK1/2, and pp38<sup>MAPK</sup>, respectively) was assessed by immunoblot. B, Expression of BMP target genes encoding Id1-Id3 was assessed by semi-quantitative RT-PCR. C, Assessment of cell proliferation in the lungs of saline- and MCT-treated rats by PCNA staining (red). Areas demarcated in (a) and (b) are magnified in (c) and (d), respectively. Arrows indicate positive PCNA staining in the smooth muscle layer of small resistance arteries. wk indicates weeks.

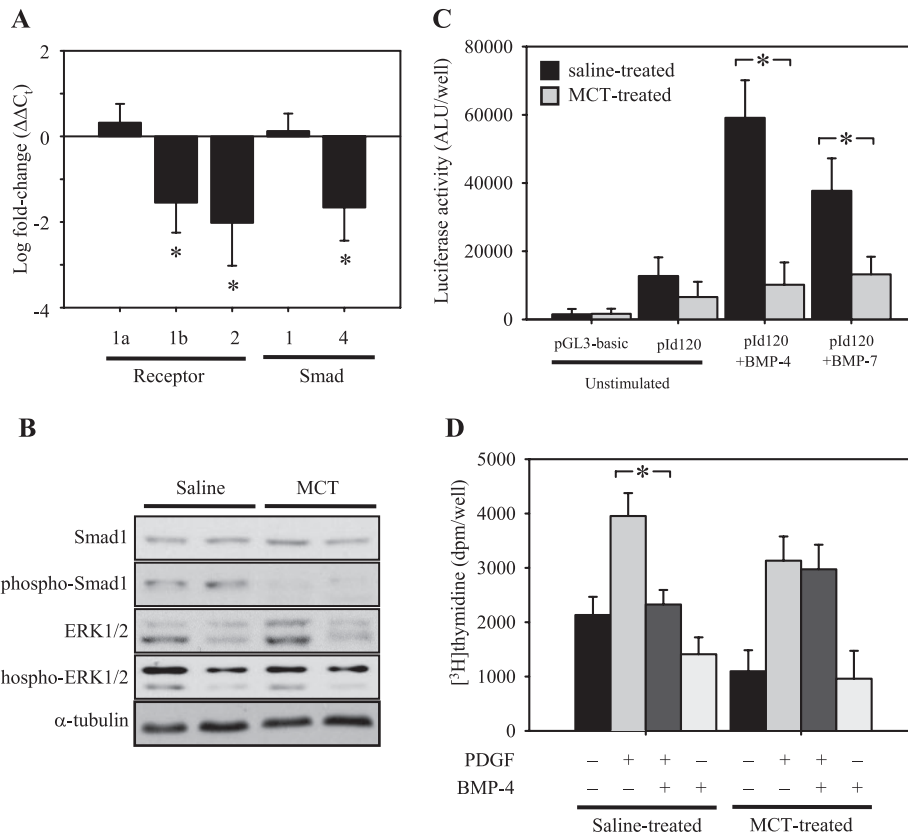


**Figure 5.** BMP signaling in PASCs from MCT-treated rats. A, Expression of BMP signaling machinery was assessed by real-time RT-PCR in PASCs from saline- and MCT-treated rats. B, BMP signaling in PASCs from saline- and MCT-treated rats assessed by immunoblot for Smad1 and ERK phosphorylation. C, Induction of a pId120 BMP/Smad-responsive promoter by BMP ligands in PASCs from saline- (black bars) and MCT-treated (gray bars) rats, 4 weeks after treatment. Expression of the control vector, pGL3-Control, was not significantly different between groups (data not shown). D, Proliferation of PASCs from saline- and MCT-treated rats was assessed by [<sup>3</sup>H]thymidine incorporation after stimulation with vehicle, PDGF, BMP-4, or combinations thereof. For C and D, data are illustrated from a single experiment, where each condition was assessed in quintuplicate, and are representative of the same trend observed over 5 independent experiments. ALU indicates arbitrary luminescent units. Values represent the mean ± SD. \*P < 0.05 between indicated groups.

treated rats exhibited a 3-fold reduction in apoptosis induced by either BMP-4 or BMP-7 (Figure 6A and 6B). Together, these proliferation and apoptosis data indicate that perturbed signaling in MCT-treated rats does have functional consequences for the maintenance of PASCs cell mass in MCT-treated rats.

### Discussion

Members of the TGF-β superfamily of growth factors are emerging as important mediators of vascular disorders, including atherosclerosis, restenosis, hereditary hemorrhagic telangiectasia, and PAH.<sup>34</sup> The BMPs and their receptors constitute an important subgroup within this superfamily, having been accredited with roles in the pathogenesis of familial and idiopathic forms of PAH.<sup>2,4</sup> We assessed the expression and function of the BMP/Smad axis in MCT-induced PAH in rats, a popularly used (albeit poorly understood) model of IPAH.<sup>16,17</sup> Our data demonstrated pronounced dysregulation of BMP/Smad signaling in MCT-induced PAH in rats, and that this perturbed signaling has functional consequences for the maintenance of PASC cell mass. The mechanism by which MCT exerts its effect remains unclear. It has been proposed that MCT treatment causes endothelial damage and changes

in the extracellular matrix composition and remodeling.<sup>16,17</sup> However, we demonstrate here that MCT also affects the airways, and PASCs from MCT-treated rats remain atypical after serial passage, suggesting that persistent changes are induced in that cell type. It could be suggested that MCT induces a transdifferentiation of PASCs into cells with an altered phenotype; however, these ideas remain entirely speculative.

In a hypoxia-induced PAH model in rats, Takahashi et al<sup>15</sup> demonstrated a downregulation of *Bmpr2* in the pulmonary arteries in response to chronic hypoxia. In whole-lung extracts from these rats, phosphorylation of p38<sup>MAPK</sup> was also reduced; however, no change in phosphorylated Smad1/5/8 was observed. These authors concluded that the BMP/MAP kinase axis, but not the BMP/Smad axis, was perturbed in hypoxia-induced PAH. Our data contrast sharply with those results, because we observed a dramatic reduction in both phosphorylated Smad1 and transcription of the BMP/Smad1-responsive genes *id1* and *id3*. In contrast, only a slight reduction in ERK1/2 phosphorylation, and no change in p38<sup>MAPK</sup> phosphorylation, was observed in whole-lung homogenates from MCT-treated rats with severe PAH. In PASCs isolated from these rats, BMP signaling was functionally impaired (as assessed by a luciferase reporter assay),

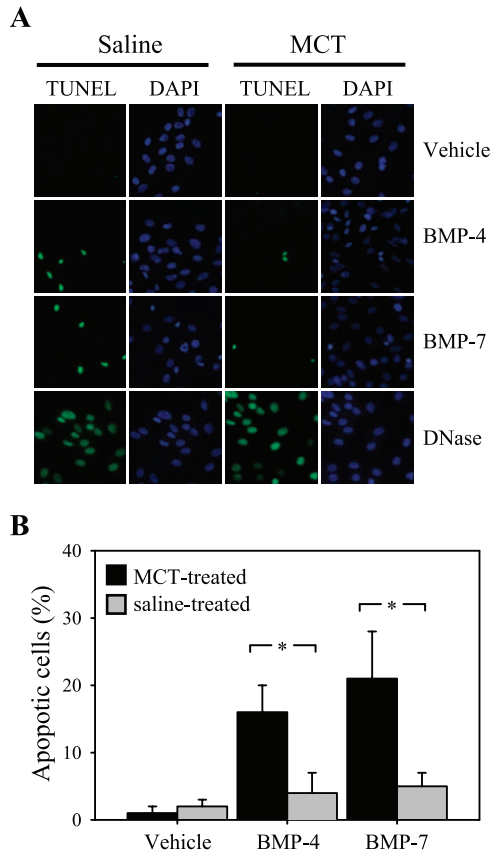


**Figure 6.** Induction of apoptosis by BMP ligands in PSMCs from saline-treated (black bars) or MCT-treated (gray bars) rats, 4 weeks after treatment, assessed by TUNEL assay. DNase served as a positive control for the TUNEL reaction. Representative fields are illustrated in A, whereas quantitation of 20 representative fields is illustrated in B. \* $P < 0.05$  between indicated groups.

and although levels of phospho-Smad1 were dramatically reduced, no change in the phosphorylation status of ERK1/2 was observed. Thus, it appears that different BMP signaling pathways are perturbed in hypoxic versus MCT-induced PAH.

Several parallels are evident, however, comparing the MCT-induced rat model of PAH with human IPAH and FPAH. Total Smad1 levels and baseline ERK1/2 phosphorylation are unchanged in PSMCs isolated from lungs from both IPAH and FPAH patients, although levels of phosphorylated Smad1 are reduced in both disorders.<sup>32,33</sup> We have observed an identical situation in MCT-induced PAH in rats. Similarly, reduced levels of both Bmpr1a<sup>11</sup> and Bmpr2<sup>10,12</sup> have been observed in lungs from patients with IPAH, and a similar pattern is observed in MCT-induced PAH in rats, particularly with respect to Bmpr2, implicating both receptors in the development of PAH. Our data are consistent with the observation that loss of functional Bmpr2 alone is not sufficient to generate a hypertensive condition, because adenoviral delivery of the *bmpr2* gene to the resistance pulmonary arteries of MCT-treated rats does not ameliorate MCT-induced PAH.<sup>35</sup> These observations are in agreement with the idea that PAH is a disease with multifactorial etiology,<sup>1-4</sup> and support proposed roles for BMP signaling in the pathogenesis of IPAH. Our data also illustrate that in the

context of BMP signaling, the MCT model appears to more closely mimic human IPAH than does the hypoxia model.

It has been proposed that the aberrant vascular remodeling observed in IPAH results from alterations to the balance in cellular responses to BMP ligands, which occur not through a global loss of BMP responsiveness, but rather through changes in the balance of different heteromeric BMP receptor complexes which can shift the balance from a growth inhibitory to a mitogenic response.<sup>36</sup> This idea has emerged, in part, from observations that ablation of *Bmpr2* in PSMCs can diminish or augment cellular responses to different BMP ligands, by promoting the formation of atypical type I–type II receptor complexes. For example, *Bmpr1a* can form complexes with an alternative type II receptor, the activin receptor IIa (*Acvr2a*),<sup>30</sup> and BMP signals can be transmitted by *Acvr1*–*Acvr2a* complexes. Neither complex forms in the presence of *Bmpr2*, and these atypical complexes exhibit peculiar BMP signaling.<sup>30</sup> The data we present in this study indicate a dramatic downregulation of *Bmpr1b* and *Bmpr2*, although only a moderate downregulation of *Acvr1* and *Acvr2a*, suggesting the possibility that in MCT-treated rats, the *Bmpr1a* is free to form alternative atypical signaling complexes with other receptors, and BMP signaling may thus be undertaken by these atypical complexes.

It has also been demonstrated that the BMP/Smad and BMP/extracellular signal regulated kinase (ERK)/p38<sup>MAPK</sup> axes have different effects on PSMCs, with the Smad axis being growth-inhibitory and the ERK/p38<sup>MAPK</sup> axis being proliferative and prosurvival. Yang et al<sup>32</sup> demonstrated that the pulmonary vasculature of patients with both familial and idiopathic PAH are deficient in the activated forms of Smad1, and proposed that defective BMP/Smad signaling, and the consequently unopposed BMP/ERK/p38<sup>MAPK</sup> signaling contributed to abnormal VSMC proliferation. Indeed, the pulmonary vascular medial hypertrophy associated with IPAH is believed to result largely from increased proliferation and decreased apoptosis of PSMCs.<sup>1</sup> Our data support a similar idea in MCT-induced PAH, where Smad phosphorylation (and thus signaling) is abolished, but ERK1/2 phosphorylation is only slightly affected in whole lung extracts, and remains unaffected in PSMCs from MCT-treated rats. This would shift the balance dramatically in favor of ERK signaling and hence proliferation and survival of PSMCs. In support of this idea, BMP ligands induce apoptosis in PSMCs from healthy volunteers. However, the ability of BMP ligands to induce apoptosis is dramatically decreased in proximal PSMCs from IPAH patients.<sup>33</sup> We illustrate here that this is also true of proximal PSMCs isolated from rats suffering from MCT-induced PAH, where BMP-4 and BMP-7 exhibited a reduced proapoptotic capacity, and consequently did not suppress PSMC growth as effectively as was observed in PSMCs from healthy saline-treated control rats.

In sum, our data illustrate that as a consequence of downregulated expression of both BMP receptors and Smad proteins, the BMP signaling capacity of the lung, and specifically of PSMCs, is impaired in MCT-treated rats. These observations have important implications for the maintenance of PSMC cell mass in the lungs of rats suffering from MCT-induced PAH. As such, our data lend solid support to

the proposed roles for BMP signaling in the pathogenesis of human PAH.

### Sources of Funding

The authors are supported by the Deutsche Forschungsgemeinschaft (SFB547 "Cardiopulmonary Circulation"), the "Excellence Cluster Cardiopulmonary System" of the universities of Giessen and Frankfurt and the Max-Planck-Institute for Heart and Lung Research in Bad Nauheim, and the European Commission Sixth European Framework Programme "Pulmotension".

### Disclosures

None.

### References

- Rubin LJ. Pulmonary arterial hypertension. *Proc Am Thorac Soc.* 2006; 3:111–115.
- Humbert M, Morrell NW, Archer SL, Stenmark KR, MacLean MR, Lang IM, Christman BW, Weir EK, Eickelberg O, Voelkel NF, Rabinovitch M. Cellular and molecular pathobiology of pulmonary arterial hypertension. *J Am Coll Cardiol.* 2004;43:13S–24S.
- Eddahibi S, Morrell N, d'Ortho MP, Naeije R, Adnot S. Pathobiology of pulmonary arterial hypertension. *Eur Respir J.* 2002;20:1559–1572.
- Eickelberg O, Yeager ME, Grimminger F. The tantalizing triplet of pulmonary hypertension-BMP receptors, serotonin receptors, and angiotensins. *Cardiovasc Res.* 2003;60:465–467.
- Miyazono K, Maeda S, Imamura T. BMP receptor signaling: transcriptional targets, regulation of signals, and signaling cross-talk. *Cytokine Growth Factor Rev.* 2005;16:251–263.
- Nohe A, Hassel S, Ehrlich M, Neubauer F, Sebald W, Henis YI, Knaus P. The mode of bone morphogenetic protein (BMP) receptor oligomerization determines different BMP-2 signaling pathways. *J Biol Chem.* 2002;277:5330–5338.
- Lane KB, Machado RD, Pauciuolo MW, Thomson JR, Phillips JA 3rd, Loyd JE, Nichols WC, Trembath RC. Heterozygous germline mutations in BMPR2, encoding a TGF-beta receptor, cause familial primary pulmonary hypertension. *Nat Genet.* 2000;26:81–84.
- Thomson JR, Machado RD, Pauciuolo MW, Morgan NV, Humbert M, Elliott GC, Ward K, Yacoub M, Mikhail G, Rogers P, Newman J, Wheeler L, Higenbottam T, Gibbs JS, Egan J, Crozier A, Peacock A, Allcock R, Corris P, Loyd JE, Trembath RC, Nichols WC. Sporadic primary pulmonary hypertension is associated with germline mutations of the gene encoding BMPR-II, a receptor member of the TGF-beta family. *J Med Genet.* 2000;37:741–745.
- Nishihara A, Watabe T, Imamura T, Miyazono K. Functional heterogeneity of bone morphogenetic protein receptor-II mutants found in patients with primary pulmonary hypertension. *Mol Biol Cell.* 2002;13:3055–3063.
- Rudarakanchana N, Flanagan JA, Chen H, Upton PD, Machado R, Patel D, Trembath RC, Morrell NW. Functional analysis of bone morphogenetic protein type II receptor mutations underlying primary pulmonary hypertension. *Hum Mol Genet.* 2002;11:1517–1525.
- Du L, Sullivan CC, Chu D, Cho AJ, Kido M, Wolf PL, Yuan JX, Deutsch R, Jamieson SW, Thistlethwaite PA. Signaling molecules in nonfamilial pulmonary hypertension. *N Engl J Med.* 2003;348:500–509.
- Atkinson C, Stewart S, Upton PD, Machado R, Thomson JR, Trembath RC, Morrell NW. Primary pulmonary hypertension is associated with reduced pulmonary vascular expression of type II bone morphogenetic protein receptor. *Circulation.* 2002;105:1672–1678.
- Song Y, Jones JE, Beppu H, Keaney JF Jr, Loscalzo J, Zhang YY. Increased susceptibility to pulmonary hypertension in heterozygous BMPR2-mutant mice. *Circulation.* 2005;112:553–562.
- West J, Fagan K, Steudel W, Fouty B, Lane K, Harral J, Hoedt-Miller M, Tada Y, Ozimek J, Tuder R, Rodman DM. Pulmonary hypertension in transgenic mice expressing a dominant-negative BMPRII gene in smooth muscle. *Circ Res.* 2004;94:1109–1114.
- Takahashi H, Goto N, Kojima Y, Tsuda Y, Morio Y, Muramatsu M, Fukuchi Y. Down-regulation of type II bone morphogenetic protein receptor in hypoxic pulmonary hypertension. *Am J Physiol Lung Cell Mol Physiol.* 2005;290:L450–L458.
- Rabinovitch M. Investigational approaches to pulmonary hypertension. *Toxicol Pathol.* 1991;19:458–469.
- van Suylen RJ, Smits JF, Daemen MJ. Pulmonary artery remodeling differs in hypoxia- and monocrotaline-induced pulmonary hypertension. *Am J Respir Crit Care Med.* 1998;157:1423–1428.
- Dumitrascu R, Weissmann N, Ghofrani HA, Dony E, Beuerlein K, Schmidt H, Stasch JP, Gnoth MJ, Seeger W, Grimminger F, Schermuly RT. Activation of soluble guanylate cyclase reverses experimental pulmonary hypertension and vascular remodeling. *Circulation.* 2006;113:286–295.
- Schermuly RT, Dony E, Ghofrani HA, Pullamsetti S, Savai R, Roth M, Sydykov A, Lai YJ, Weissmann N, Seeger W, Grimminger F. Reversal of experimental pulmonary hypertension by PDGF inhibition. *J Clin Invest.* 2005;115:2811–2821.
- Alejandro-Alcázar MA, Kwapiszewska G, Reiss I, Amarie OA, Marsh LM, Sevilla-Pérez J, Wygrecka M, Eul P, Köbrich S, Hesse M, Schermuly RT, Seeger W, Eickelberg O, Morty RE. Hyperoxia modulates TGF-beta signaling in a mouse model of bronchopulmonary dysplasia. *Am J Physiol Lung Cell Mol Physiol.* 2006;292:L537–L549.
- Kwapiszewska G, Wilhelm J, Wolff S, Laumanns I, Koenig IR, Ziegler A, Seeger W, Bohle RM, Weissmann N, Fink L. Expression profiling of laser-microdissected intrapulmonary arteries in hypoxia-induced pulmonary hypertension. *Respir Res.* 2005;6:109.
- Vadász I, Morty RE, Olschewski A, Konigshoff M, Kohstall MG, Ghofrani HA, Grimminger F, Seeger W. Thrombin impairs alveolar fluid clearance by promoting endocytosis of Na<sup>+</sup>,K<sup>+</sup>-ATPase. *Am J Respir Cell Mol Biol.* 2005;33:343–354.
- Gilboa L, Nohe A, Geissendorfer T, Sebald W, Henis YI, Knaus P. Bone morphogenetic protein receptor complexes on the surface of live cells: a new oligomerization mode for serine/threonine kinase receptors. *Mol Biol Cell.* 2000;11:1023–1035.
- Seay U, Sedding D, Krick S, Hecker M, Seeger W, Eickelberg O. Transforming Growth Factor-beta-Dependent Growth Inhibition in Primary Vascular Smooth Muscle Cells Is p38-Dependent. *J Pharmacol Exp Ther.* 2005;315:1005–1012.
- Brevnova EE, Platoshyn O, Zhang S, Yuan JX. Overexpression of human KCNA5 increases IK<sub>v</sub> and enhances apoptosis. *Am J Physiol Cell Physiol.* 2004;287:C715–C722.
- Lopez-Rovira T, Chalaux E, Massagué J, Rosa JL, Ventura F. Direct binding of Smad1 and Smad4 to two distinct motifs mediates bone morphogenetic protein-specific transcriptional activation of Id1 gene. *J Biol Chem.* 2002;277:3176–3185.
- Mitani Y, Ueda M, Maruyama K, Shimpo H, Kojima A, Matsumura M, Aoki K, Sakurai M. Mast cell chymase in pulmonary hypertension. *Thorax.* 1999;54:88–90.
- Goto J, Ishikawa K, Kawamura K, Watanabe Y, Matumoto H, Sugawara D, Maruyama Y. Heme oxygenase-1 reduces murine monocrotaline-induced pulmonary inflammatory responses and resultant right ventricular overload. *Antioxid Redox Signal.* 2002;4:563–568.
- ten Dijke P, Korchynskyi O, Valdimarsdottir G, Goumans MJ. Controlling cell fate by bone morphogenetic protein receptors. *Mol Cell Endocrinol.* 2003;211:105–113.
- Yu PB, Beppu H, Kawai N, Li E, Bloch KD. Bone morphogenetic protein (BMP) type II receptor deletion reveals BMP ligand-specific gain of signaling in pulmonary artery smooth muscle cells. *J Biol Chem.* 2005; 280:24443–24450.
- Morrell NW, Yang X, Upton PD, Jourdan KB, Morgan N, Sheares KK, Trembath RC. Altered growth responses of pulmonary artery smooth muscle cells from patients with primary pulmonary hypertension to transforming growth factor-beta(1) and bone morphogenetic proteins. *Circulation.* 2001;104:790–795.
- Yang X, Long L, Southwood M, Rudarakanchana N, Upton PD, Jeffery TK, Atkinson C, Chen H, Trembath RC, Morrell NW. Dysfunctional Smad signaling contributes to abnormal smooth muscle cell proliferation in familial pulmonary arterial hypertension. *Circ Res.* 2005;96:1053–1063.
- Zhang S, Fantozzi I, Tigno DD, Yi ES, Platoshyn O, Thistlethwaite PA, Kriett JM, Yung G, Rubin LJ, Yuan JX. Bone morphogenetic proteins induce apoptosis in human pulmonary vascular smooth muscle cells. *Am J Physiol Lung Cell Mol Physiol.* 2003;285:L740–L754.
- Bobik A. Transforming Growth Factor-betas and Vascular Disorders. *Arterioscler Thromb Vasc Biol.* 2006;26:1712–1720.
- McMurtry MS, Moudgil R, Hashimoto K, Bonnet S, Michelakis ED, Archer SL. Overexpression of human bone morphogenetic protein receptor II does not ameliorate monocrotaline pulmonary arterial hypertension. *Am J Physiol Lung Cell Mol Physiol.* In press.
- Frank DB, Abtahi A, Yamaguchi DJ, Manning S, Shyr Y, Pozzi A, Baldwin HS, Johnson JE, de Caestecker MP. Bone morphogenetic protein 4 promotes pulmonary vascular remodeling in hypoxic pulmonary hypertension. *Circ Res.* 2005;97:496–504.

Supplementary online information for:

Dysregulated bone morphogenetic protein signaling in monocrotaline-induced pulmonary arterial hypertension

**Rory E. Morty, Bozena Nejman, Grazyna Kwapiszewska, Matthias Hecker, Anka Zakrzewicz, Fotini M. Kouri, Dorothea M. Peters, Rio Dumitrascu, Werner Seeger, Petra Knaus, Ralph T. Schermuly, and Oliver Eickelberg**

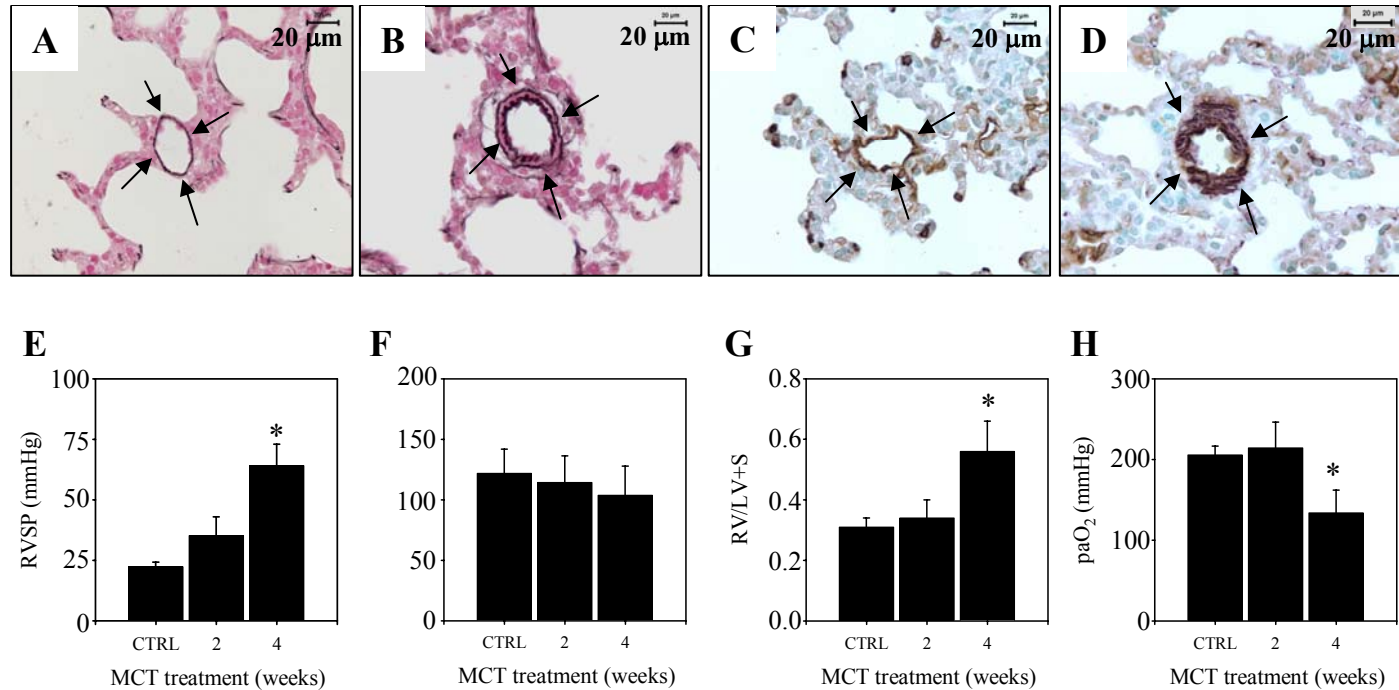
*Department of Internal Medicine, University of Giessen Lung Center, Justus Liebig University, Giessen, Germany; and the Institute of Chemistry and Biochemistry, Free University of Berlin, Berlin, Germany*

This online supplement consists of one table (Supplementary Table I) and four figures (Supplementary Figure I - Supplementary Figure IV).

Supplementary Table I. Primers employed for RT-PCR. Forward and reverse primers are indicated for real-time (rt) and semi-quantitative (sq) PCR reactions.

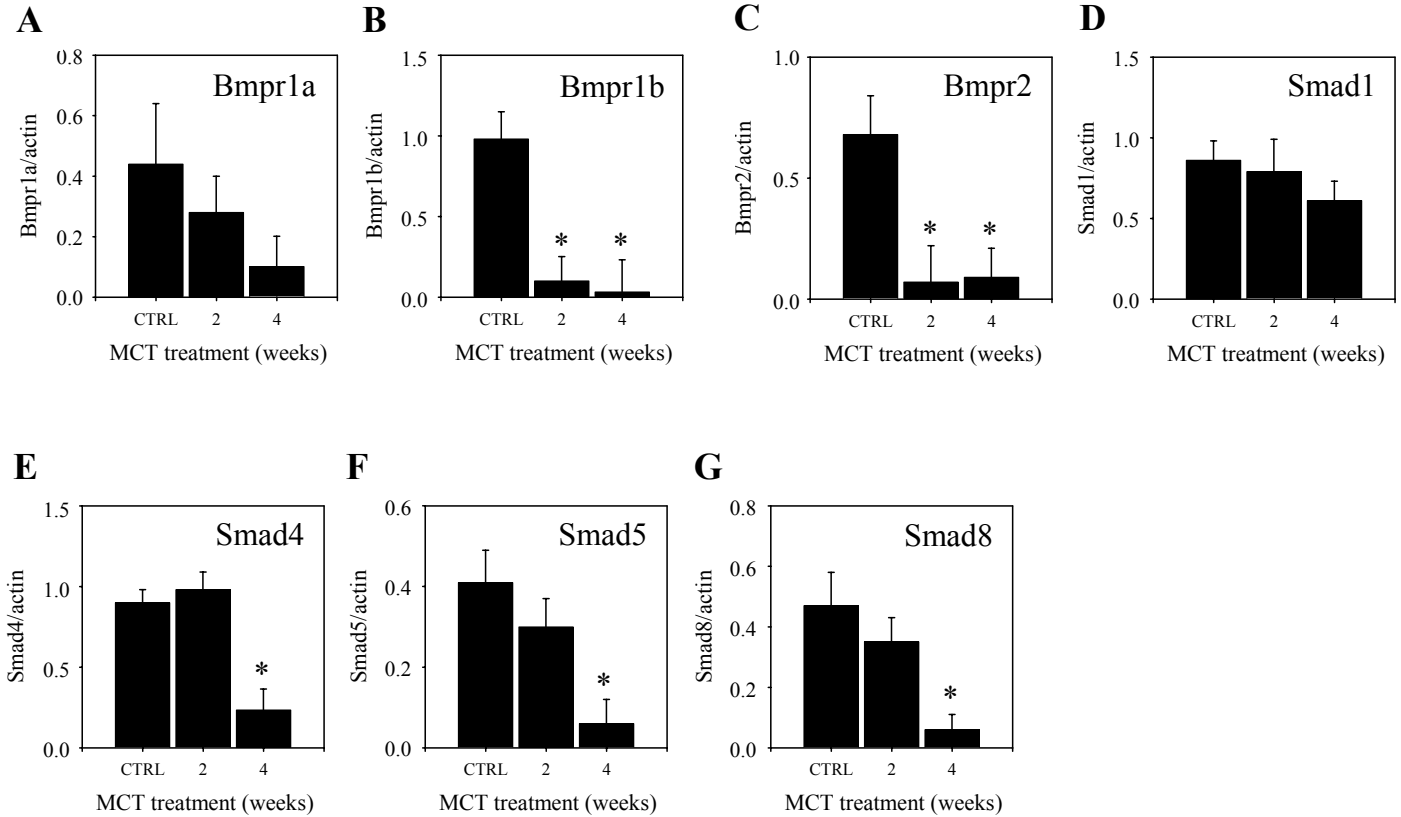
Gene	Forward Primer	Reverse Primer	Number of cycles	Annealing temperature (°C)	Amplicon size (bp)
<i>actb</i> (sq)	5'-CTAAGGCCAACCGTGAAAAG-3'	5'-CTTCTGCATCCTGTGACGAA-3'	20	62.0	611
<i>acvr1</i> (rt)	5'-TCATGCTGTTTGGCACAGAT-3'	5'-CATACTCGGGGAAGGGAGAG-3'	45	61.0	129
<i>acvr2a</i> (rt)	5'-AAGGTTGTTGGCTGGATGAT-3'	5'-CACATATTGCCCTCACAGCA-3'	45	60.0	154
<i>bmpr1a</i> (rt)	5'-TAGCACCAGAGGACACCTTACCT-3'	5'-TGGCAAAGCAATGGCCAT-3'	45	60.0	106
<i>bmpr1a</i> (sq)	5'-AAGAAGCCGAAAAATGGAGT-3'	5'-CGCCATTTACCCATCCATAC-3'	28	56.5	638
<i>bmpr1b</i> (rt)	5'-GTGGCGTGGAGAAAAGGTAG-3'	5'-CAAGACCCAGTCCCTTTGAT-3'	45	60.0	150
<i>bmpr1b</i> (sq)	5'-TGCACAGAAAGGAACGAATG-3'	5'-CAGCATGGACTTGGCATCTA-3'	25	59.0	621
<i>bmpr2</i> (rt)	5'-TCTGTGGGAGAAATCAAAAAGGG-3'	5'-GCAGCAAAAACGGTATGTTCC-3'	45	60.0	148
<i>bmpr2</i> (sq)	5'-GACTTCACACAGGCTGCAAA-3'	5'-ATCCAGAGAATTGGGCCTCT-3'	32	62.0	663
<i>cma1</i> (rt)	5'-GGATGAATCTCCATGCTCTGT-3'	5'-CGGGAGTGTGGTATGCACT-3'	45	60.0	100
<i>cma1</i> (sq)	5'-CGAAACTTTGTGCTGACTGC-3'	5'-TGCATTCGGATGTACGTAGG-3'	34	59.5	501
<i>gapdh</i> (sq)	5'-TGGTGAAGGTCCGGTGTGAACG-3'	5'-CGCCTGCTTACCACCTTCTT-3'	22	59.5	788
<i>hmbs</i> (rt)	5'-CCCACGCGAATCACTCTCAT-3'	5'-TGTCTGGTAACGGCAATGCG-3'	45	60.0	118
<i>hmox1</i> (rt)	5'-CACAGCTCGACAGCATGTCC-3'	5'-ACCCTTCTGAAAGTTCCTCA-3'	45	60.0	110
<i>hmox1</i> (sq)	5'-TGATGGCCTCCTTGATACCAT-3'	5'-TGCTGATCTGGGATTTTCCT-3'	26	62.5	633
<i>hspa8</i> (sq)	5'-CGGCCAAGAATCAGGTTGCA-3'	5'-ATGTCAGACTGAACAACAGC-3'	21	62.0	100
<i>id1</i> (rt)	5'-AGTGGTGTCTGGTCTGTGCG-3'	5'-GCTCCTTGAGGCGTGAGTAG-3'	45	60.0	126
<i>id1</i> (sq)	5'-TGCAGCGCGCAGTGTGAGTGC-3'	5'-TCAGCGACACAAGATGCGGTC-3'	21	58.0	488
<i>id2</i> (rt)	5'-CCAGAGACCTGGACAGAACC-3'	5'-CGACATAAGCTCAGAAGGGAAT-3'	45	60.0	132
<i>id2</i> (sq)	5'-ATGAAAGCCTTCAGTCCGGTG-3'	5'-TTAGCCACAGAGTACTTTGCT-3'	21	59.0	408
<i>id3</i> (rt)	5'-CCTCGACCTTCAAGTGGTTC-3'	5'-CAGTGGCAAAAACCTCTTG-3'	45	60.0	124
<i>id3</i> (sq)	5'-ATGAAGGCGCTGAGCCCGGTG-3'	5'-TCAGTGGCAAAAACCTCTT-3'	21	61.5	354
<i>smad1</i> (rt)	5'-TGTTCCAAGCAGAAGGAAAG-3'	5'-TGAGGGTTGTAAGTCTGCTGTG-3'	45	60.0	121
<i>smad1</i> (sq)	5'-GAAACAGGGCGACGAAGAA-3'	5'-AACCATCCACCAACACGCT-3'	25	58.5	845
<i>smad4</i> (rt)	5'-CTCACCCAGCAAGTGTGTC-3'	5'-CTCCACAGACGGGCATAGAT-3'	45	60.0	116
<i>smad4</i> (sq)	5'-CCACCAACTTCCCAACAT-3'	5'-CCAGGACCAGGGATGTTTC-3'	24	57.0	787
<i>smad5</i> (rt)	5'-TGTGAGTTTCTTTTGGATCG-3'	5'-TGACGAGGCACCTAACAAGTGG-3'	45	60.0	98
<i>smad5</i> (sq)	5'-AGTCCAGCCGTGAAGCGATTG-3'	5'-GATGTGCCGCCTGGTGTCTC-3'	27	58.5	957
<i>smad6</i> (rt)	5'-GAGCTGAAACCCCTGTGCGG-3'	5'-GGCGGCGATTCTGGCCCGCAGAG-3'	45	60.0	110
<i>smad6</i> (sq)	5'-GTGTTGCAACCCCTACCACT-3'	5'-GGCAGGAGGTGATGAACTGT-3'	26	56.0	722
<i>smad7</i> (rt)	5'-GCATTCTCGGAAGTCAAGA-3'	5'-GAGGAAGGTACAGCGTCTGG-3'	45	60.0	117
<i>smad7</i> (sq)	5'-TCCCCCTCCTTACTCC-3'	5'-GAACTCGTGGTCATTGGGC-3'	27	58.5	540
<i>smad8</i> (rt)	5'-GAGTTCCCGTTTGGCTCTAA-3'	5'-AGGCTGAGCTGAGGGTTGTA-3'	45	60.0	106
<i>smad8</i> (sq)	5'-CACAGCGAGTACAACCTCA-3'	5'-CGTGCACATCTTCGTGAGTT-3'	29	59.5	702
<i>tuba1</i> (sq)	5'-TCTTCCACCAGAACAGCTT-3'	5'-TTGGTGATCTCTGCCACTGA-3'	21	63.0	622

# Supplementary Figure I



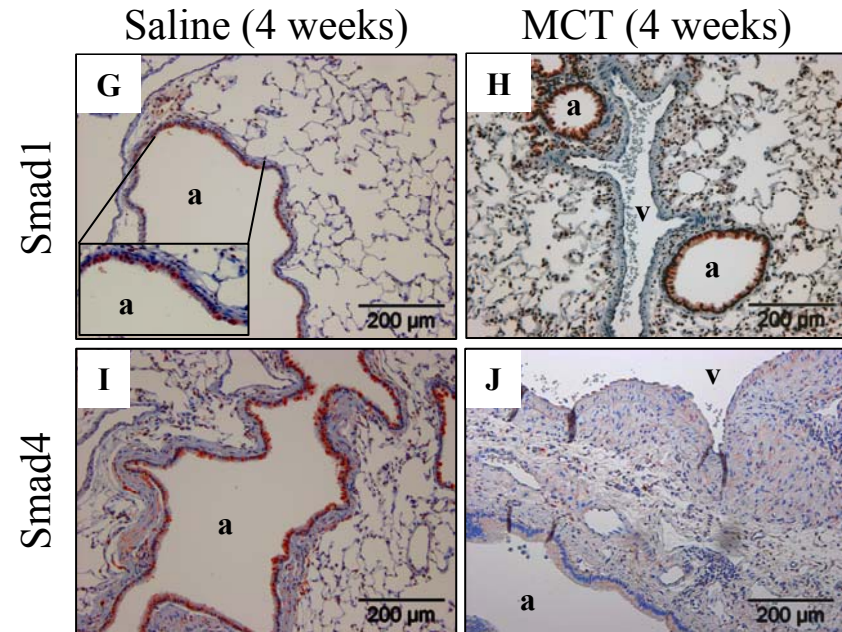
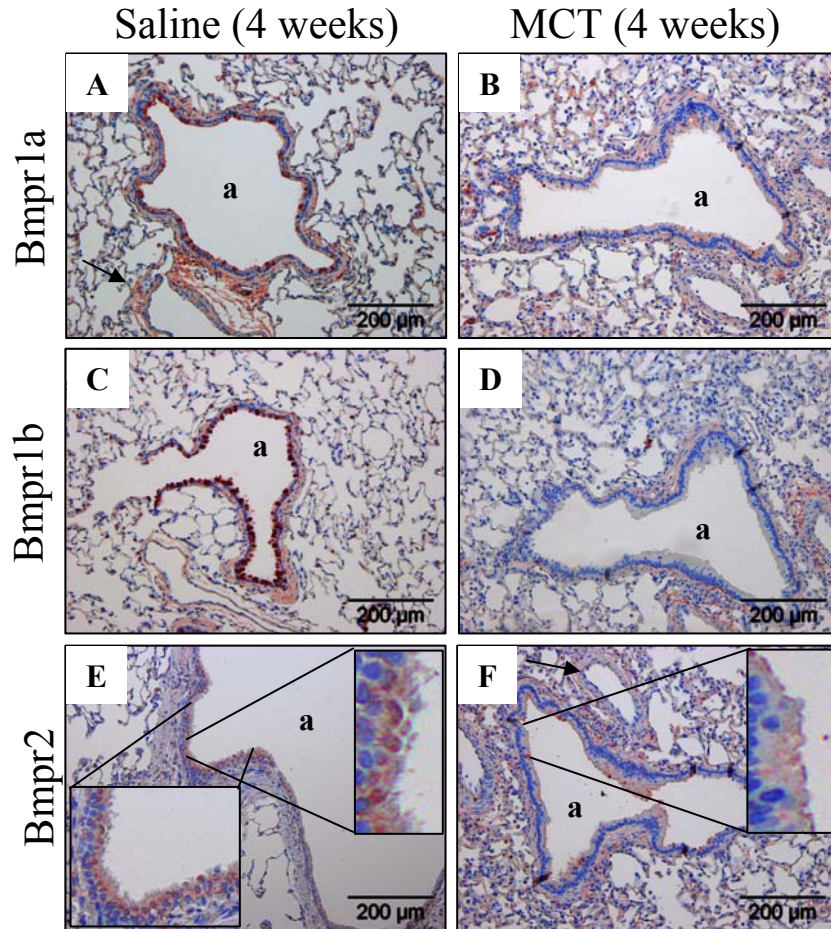
**Supplementary Figure I.** Monocrotaline induces pulmonary arterial hypertension and vascular remodeling in rats. Elastin staining (A and B) and dual-staining for von Willebrand factor (brown) and smooth muscle actin (purple) (C and D) in small pulmonary arteries (indicated by arrows) in 3  $\mu$ m sections prepared from the lungs of rats four weeks after administration of vehicle alone (A and C), or monocrotaline (B and D). (E) Right ventricular systolic pressure (RVSP), (F) systemic arterial pressure (SAP), (G) right ventricle-to-left ventricle+septum ratio (RV/LV+S), and (I) partial pressure of oxygen in arterial blood (paO<sub>2</sub>) were determined in control rats, four weeks after saline administration, and in monocrotaline-treated rats, two and four weeks after monocrotaline administration. \*,  $p < 0.05$ , relative to controls

# Supplementary Figure II



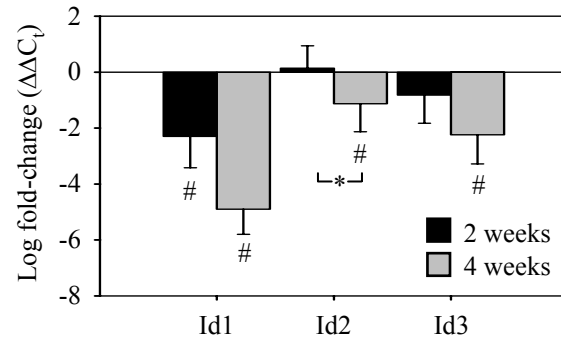
**Supplementary Figure II.** Expression of BMP signaling machinery in MCT-treated rats assessed by immunoblot. These data represent the quantitation of immunoblot data is illustrated in Figure 1. \*,  $p < 0.05$ , relative to controls. CTRL, control.

# Supplementary Figure III



**Supplementary Figure III.** Localization of BMP receptors and Smad proteins in the airways of MCT-treated rats. BMP receptors and Smads were localized (red color) in the airways (a) and vessels (v) of saline- and MCT-treated rats.

# Supplementary Figure IV



**Supplementary Figure IV.** Expression of BMP target genes encoding Id1-Id3 was assessed in lungs from MCT-treated rats by real-time RT-PCR (black bars, two weeks; gray bars, four weeks, relative to saline-treated controls). wk, weeks. #,  $p < 0.05$ , relative to saline treated controls; \*,  $p < 0.05$ , between indicated groups.